

mOptical Sensing for the Internet of Things: A Smartphone-Controlled Platform for Temperature Monitoring

João F. C. B. Ramalho, Luís D. Carlos, Paulo S. André, and Rute A. S. Ferreira*

Sensors play a key role on the Internet of Things (IoT), providing monitoring inside and outside the networks in a multitude of parameters. A fundamental parameter to sense is temperature, being essential to acquire knowledge on the best way to include thermal sensing into the communications networks. Despite that the temperature measurement in the optical domain is well known for its advantages compared with the electric one, its incorporation in the IoT is a challenge due to the lack of affordable strategies able to convert optical into an electronic signal in a cost-effective way. The coupling of such optical sensors to smartphones appears as an exciting strategy for mobile optical (mOptical) sensing. Herein, advances in optical temperature sensors for mOptical sensing are reviewed and the chronological mechanistic context of waveguided and nonguided optical signal sensors is outlined. A new path for advances in photonics research is traced, established by the incorporation of smartphones as a tool in science and engineering that foresees new designs for mOptical temperature sensor toward IoT.

1. Introduction

The Internet of Things (IoT) was introduced in 1999 and ever since it has been re(de)efined with trends, elements, and definitions surveyed and discussed over the years (2010,^[1] 2013,^[2] 2015,^[3] and 2019^[4]). Today it is no longer an idea of the future and has become a concept of the present, beginning to be incorporated in our daily life and extending to all sorts of branches in society, including industry 4.0,^[5] healthcare 4.0,^[6] and smart

cities.^[7] In a simplified way, IoT can be defined as a network of entities connected to each other's exchanging information. For IoT to become a functional network, several technologies will play a key role and work together combining information and communication technologies, such as cloud, edge, and fog computing,^[8,9] big data, artificial intelligence,^[8,9] machine learning,^[10,11] cybersecurity and access control technologies,^[12] or data transmission^[13] with physical technologies as efficient energy-harvesting technologies^[14–17] or sensors,^[18,19] resulting in cyberphysical systems.


Over the past years, several developments and innovations in hardware and software increased the complexity and heterogeneity of the networks with the concomitant increase in the volume of data generated and collected. One of the main

data sources are sensors, that are present almost everywhere, monitoring different parameters within the network or on its surrounding, either in continuous mode or occasionally after the interaction. Examples include biometrics sensors (e.g., facial recognition), human behavior sensors (e.g., touch screen), device status sensors (e.g., battery, network connections), emergency events sensors (e.g., stress/fatigue, flame), and environment sensors (e.g., humidity, temperature), among others.^[20–23] Thus, the IoT comprises a large and complex network with branches reaching almost every point of science evidenced in the large number of publications in the recent years, with several reviews and surveys exploring small portions of this ubiquitous network being made.^[8–17,21,22] Among the distinct sensing technologies, optical sensors appear as real alternatives to electronic ones due to their inherent features such as contactless, large-scale measures, faster response times, immunity to electromagnetic fields,^[24] which in some scenarios are more advantageous.^[25] Temperature is one of the most demanded sensing targets, in science and in the global economy, where sensors account for $\approx 80\%$ of the world sensor market, expecting that the sector reaches economic record by 2023.^[26]

This work focuses on temperature optical sensors inserted into an IoT network. It begins with an overview of the field based on more than 11 600 publications in the past 20 years (see Section 5 for more information) revealing that optical temperature sensors may be split into two main clusters, namely waveguided optical sensors (Cluster I) and nonguiding optical

J. F. C. B. Ramalho, Prof. L. D. Carlos, Prof. R. A. S. Ferreira
Department of Physics and CICECO - Aveiro Institute of Materials
University of Aveiro
3810-193 Aveiro, Portugal
E-mail: rferreira@ua.pt

Prof. P. S. André
Department of Electrical and Computer Engineering and Instituto de
Telecomunicações
Instituto Superior Técnico
Universidade de Lisboa
1049-001 Lisbon, Portugal

 The ORCID identification number(s) for the author(s) of this article can be found under <https://doi.org/10.1002/adpr.202000211>.

© 2021 The Authors. Advanced Photonics Research published by Wiley-VCH GmbH. This is an open access article under the terms of the Creative Commons Attribution License, which permits use, distribution and reproduction in any medium, provided the original work is properly cited.

DOI: 10.1002/adpr.202000211

sensors (Cluster II). The search was refined to focus on smartphone-based optical temperature sensors, revising the current advances and trends for **m**Optical sensing. Emphasis is given to examples related to nonwaveguided optical signals due to the recent explosion of the field.

2. Optical Temperature Sensors Overview

The wide spreading of **m**Optical sensors as a reliable alternative in thermal sensing requires the identification of the vectors for the appropriate direction of the efforts toward incorporation in IoT and improved societal impact. A literature review over the past 20 years including published articles, letters, reviews, and books from Web of knowledge Collection was carried out using search keywords as temperature, sensing, and optical (see Experimental Section for more information), emanates two main clusters of sensors, namely waveguided optical sensors (Cluster I) and nonguiding optical sensors (Cluster II), **Figure 1**. Cluster I, identified with the red color, aggregates indexing terms, such as fiber Bragg grating,^[27] interferometer (Fabry–Perot, Sagnac, or Mach–Zehnder),^[28] that are associated with waveguide

propagation of the optical signal in fiber. The indexing terms refer to either the measured property of the optical signal (e.g., polarization, reflectance spectrum, wavelength shift, intensity), the principle of operation (e.g., interferometer), or the measurand (e.g., refractive index, strain, temperature). Cluster II, represented with the green color, combine indexing terms more often associated with nonguided optical signal properties (e.g., emission spectra, fluorescent intensity ratio), the principle of operation (e.g., upconversion, downshifting), or the measurand (mainly temperature). There are indexing terms (identified in blue) that are shared by both clusters, which include, spectra, intensity, or phase, which are related to the way the temperature information is encoded into the optical signal. All the terms used to build Figure 1 are shown in Table S1, Supporting Information.

Additional information retrieved from Figure 1 appears when the data are seen from a historical temporal point of view. It is chronologically clear that in the field of optical temperature sensors, the nonguided optical signal propagation sensors (Cluster II) are a hot topic, with a higher number of publications and average citations in the past 5 years (more information in Figure S1 and Table S1, Supporting Information). Despite this,

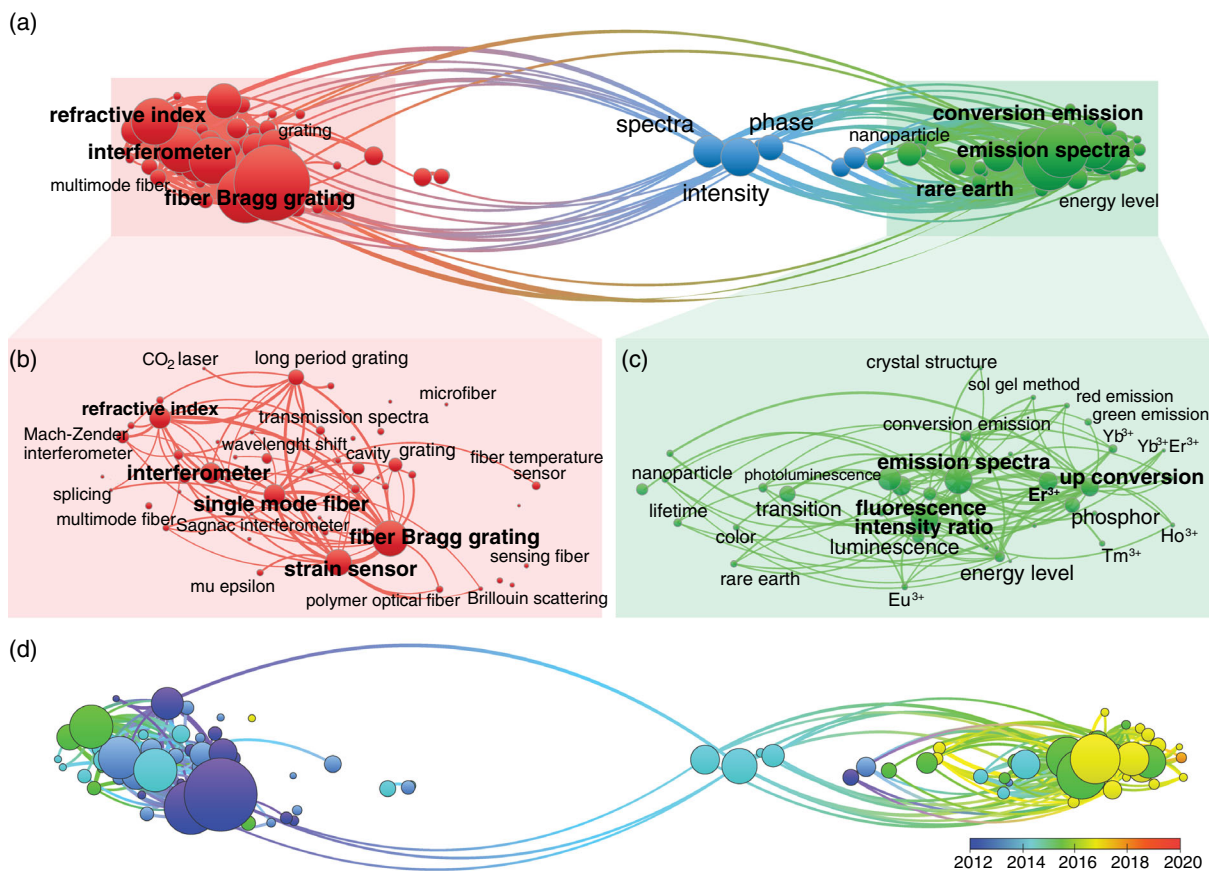


Figure 1. a) Map generated using data (title and abstract) in 11 692 publications from Web of Knowledge principal collection in the period 1999–2021, using search keywords related to temperature sensing and optical, accessed on February 4, 2021. The red and green clusters, expanded in (b) and (c), aggregate the indexing terms in (b) waveguided optical signal temperature sensors (Cluster I) and (c) nonguided optical signal temperature sensors (Cluster II). The diameter of the circles is directly proportional to the number of occurrences of an indexing term, the width of the linking line is directly proportional to the relation between them (larger width link \Rightarrow stronger relation), as well as the distance on the map (the closer two indexing terms are the more related they are). d) Chronological evolution of the map in (a).

waveguiding optical sensors are more mature and closer to daily life applications mostly due to 1) the maturity of the fiber-optic communication industries; 2) the longevity of the field with publications dating back to the 1980s, and 3) the advances in optoelectronics that allowed an easier transition from optics to electronics.^[29]

Noticeable, in Cluster I, the waveguided optical signal sensors working principle is somehow general among the different types of sensors. It is based on the propagation of the optical signal inside a medium (e.g., optical fiber), that will suffer a perturbation, being reflected, transmitted, or scattered and afterward collected and processed. In the presence of a physical disturbance (temperature, humidity, pressure, strain, etc.), the optical signal will undergo a variation, such as a wavelength (frequency) shift of the spectrum, a variation of the amplitude, changes in the polarization or phase, which constitute the sensing parameter. Thus, the sensor response is based on the mismatch between perturbed and nonperturbed conditions that are correlated with the physical disturbance applied to sense the surrounding environment.^[29–31] Many works have been published in this field, featuring improvements in the figures of merit, cost, and energy consumption reduction, and ease in manufacturing. Examples include, the fabrication of optical fibers with different materials and geometries, novel fibers working as amplifiers, multicore fibers, multiplexing schemes, or new detection systems.^[32–34]

Considering Cluster II based on nonguided optical signal sensors, their prominence started around 2015 (Figure 1d), using thermal-sensitive optical properties of the materials such as reflection, absorption, Raman scattering, or luminescence. Among those optical properties, luminescence is the one that has been drawing larger attention for thermal sensing.^[35,36] The current interest in luminescence thermometry is well evidenced in a series of very recent review papers.^[26,37–42] Luminescence is a noninvasive spectroscopic method for temperature measurement based on the thermal dependence of the phosphor emission (also known as the thermometric parameter) combining high relative thermal sensitivity ($S_r > 1\%K^{-1}$) and spatial resolution (10^{-6} m) with short acquisition times ($< 10^{-3}$ s).^[26,35,36,43–48] The working principle of luminescence thermometry is based on the temperature dependence of the materials' emission that manifests itself mostly through the 1) variation in the lifetime of a certain excited energy level, 2) emission peak shift or, the most used 3) variation in the emission intensity (I) of one or two electronic (I_1 and I_2) transitions, **Figure 2.**^[26,35–37]

Lifetime-based measurements present several advantages over the other luminescence thermometry principles, such as not being affected by the size, geometry, or concentration of the sensing probe, or by unrelated optical effects (e.g., light scattering or intensity fluctuations). As a disadvantage, it is heavily time-consuming and equipment dependent, requiring a pulsed excitation source rendering it difficult for IoT applications, nonetheless technological advances to simplify and reduce costs are being made.^[26,36]

The use of the temperature-dependent emission peak shift generally produces thermometers with a low relative sensitivity as the peak shift values are around a few dozens of cm^{-1} over a broad temperature range^[49,50] as, for example, a Tm^{3+} -doped crystalline TiO_2 film displayed a spectral shift of 1.25 nm in

CONTACTLESS TEMPERATURE SENSING

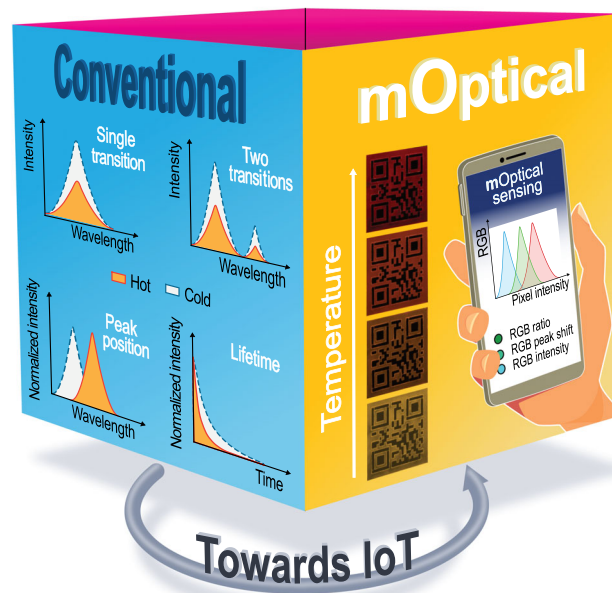


Figure 2. Schematic of the thermometric parameters (lifetime variation of a certain excited energy level, emission peak shift, and variation in the emission intensity of one or two electronic transitions) used in luminescence thermometry and those (photographs) used for **mOptical** sensing toward IoT.

the 85–750 K range. This is not, however, a rule of thumb as recently a Green Fluorescent Protein-based thermometer displays a 3 nm shift over a much shorter temperature range (293–333 K).^[51] In any way, such thermometers require in general high spectral resolution spectrometers, making difficult a practical application. Nevertheless, and as an advantage, they do not rely on an absolute intensity analysis and are not affected by intensity fluctuations caused by changes in the local concentration of the emission centers. In addition, a spectral shift-based thermometer could be useful in combination with another type of luminescent thermometers (dual sensing) to reduce experimental uncertainties.^[26,36]

The most popular approach to determine the absolute temperature is to measure the intensity ratio of distinct spectral regions in the emission spectrum (so-called self-reference ratiometric thermometer).^[52] These thermometers offer consistent temperature measurements, as they are not affected by local intensity fluctuations (e.g., emitting centers concentration or excitation source power). However, recent works have drawn attention to reliability issues caused by experimental artifacts and even intrinsic effects.^[47,53–58] The solution lies in primary thermometers, characterized by a well-established state-equation that directly relates a particular measured value to the absolute temperature without the need for calibration. So far, only a few primary luminescent thermometers have been reported,^[43,53,58–65] most of which based on the intensity ratio between two thermally coupled electronic levels, for instance, the $Er^{3+} \ ^2H_{11/2}$ and $^4S_{3/2}$ levels. In

this case, the thermometric parameter is based exclusively upon the validity of the Boltzmann distribution.^[62] The required use of spectrometers to record luminescence imposes an innovative transformation that allows primary thermometers to be useful in IoT.

In all the cases, luminescence dependence with temperature is expressed through the so-called thermometric parameter (Δ). For ratiometric thermometers, the most common example is^[52]

$$\Delta = \frac{I_1}{I_2} \quad (1)$$

The quantitative figures of merit used to characterize luminescent thermometers are the relative sensitivity (S_r), defined as the rate of change of the thermometric parameter (Δ) in response to temperature stimuli ($\partial\Delta/\partial T$) divided by the thermometric parameter (usually expressed in $\%K^{-1}$)^[35,52]

$$S_r = \frac{1}{\Delta} \left| \frac{\partial\Delta}{\partial T} \right| \quad (2)$$

and the temperature uncertainty (∂T), which is the minimum temperature change, able to be detected by the thermometer given by^[35,52]

$$\delta T = \frac{1}{S_r} \frac{\delta\Delta}{\Delta} \quad (3)$$

where $\delta\Delta$ is the uncertainty in Δ . The operating temperature range of the device, defined as the interval in which the temperature changes are larger than the uncertainty of the thermometer, is also a critical parameter.^[42] **Figure 3a** (and Table S2, Supporting Information) shows examples of the largest S_r values (S_m) reported for ratiometric (hollow symbols) luminescent thermometers with an operating range compatible with **mOptical** sensing and for smartphone-based luminescence thermometry (solid symbols).^[46,55,59,66–89] The S_r values for primary luminescent thermometers are shown in **Figure 3b**.^[43,53,58–64] Noticeable, only one example refers to smartphone-based luminescence thermometry, and presents the largest S_r value.^[59]

Based on **Figure 1**, we propose to divide the field of optical thermometry into the above mentioned two main clusters

(waveguided optical signal and nonguided optical signal), where none of each cluster permits to identify a dominant position in what concerns IoT and **mOptical** sensing with very few reports combining thermal sensing with an explicitly IoT connection and most of the examples refer only to a potential IoT link (**Table 1**), meaning that the field of optical temperature in the context of IoT is still in the infancy.

3. Optical Temperature Sensors for the IoT

In the framework of IoT, several entities are required to be connected to each other's and to the internet, exchanging information.^[4] Among those entries, sensors could play a special role. In particular, a sensor which is, in its simplest definition, a converter of external stimulate (chemical, physical) to an electronic or optical signal, generating information that is afterward processed and in the IoT context is also exchanged with the network. For electronic sensing, there is a plethora of processing and communications mechanisms, but for optical sensors, this is not so evident. To render clear our vision, an optical temperature sensor for IoT can be taken as a technology whose sensing process generates information that can be processed or transmitted to a commercially available device with an interface connected to a communication network. Several reports point to smartphones as a key element in the development of **mOptical** sensors toward IoT. In particular, for optical temperature sensors, it might be the main path, as smartphones are a ubiquitous technology, with the necessary processing capacity and, most importantly, they can convert optics into electronics due to the charge-coupled device (CCD) camera.^[90–92] Based on this definition, examples found in the literature comprehending both waveguided and nonguided optical signal thermometers, prospecting the first steps to **mOptical** temperature sensing into IoT are presented.

3.1. Waveguided Optical Signal Temperature Sensors (Cluster I)

Cluster I sensors in IoT make use of an optical fiber attached to the smartphone camera. Depending on the effect of the temperature, the disturbance created on the guided light can result in either an intensity variation^[79,80] or a spectral shift.^[93] In the

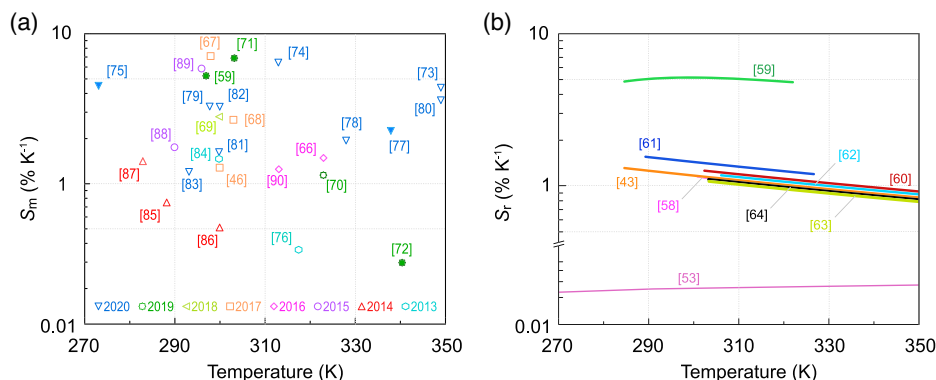


Figure 3. a) Recent examples of S_m values for ratiometric luminescent thermometers (hollow symbols) operating in a temperature range suitable for **mOptical** sensing and for smartphone-based luminescence thermometry (solid symbols). b) Relative sensitivity values as function of the temperature for primary luminescent thermometers.

Table 1. Highlights and figures of merit of selected examples temperature sensors using smartphones. The mechanism, thermometric parameter, input (experimental temperature-dependent raw data), operation range, the ability to communicate with the IoT environment, maximum relative sensitivity (S_r), and minimum temperature uncertainty (∂T) are listed.

Mechanism	Thermometric parameter	Input	Operating range [K]	IoT link	S_r [%K ⁻¹]	∂T [K]	Ref.	
SPR	Intensity ratio	Photograph (Grayscale)	263–453	No	$\approx 0.27^a$	–	[80]	
Macrobending		Photograph (RGB)	293–393	No	$\approx 6.74^a$	–	[79]	
Optical path difference of thin film	Reflectance spectrum shift	Photograph (Grayscale)	303–340	No	$\approx 0.07^a$	–	[93]	
Luminescent	Emission spectrum shift	Emission spectrum	303–393	No	$\approx 0.06^a$	–	[98]	
		Intensity difference	Photograph (RGB)	303–418	Yes	0.164 K^{-1b}	–	[99]
	Intensity ratio	Emission spectrum	278–408	No	3.40	–	[97]	
				298–338	No	2.17	–	[84]
		Photograph (CIE)	298–425	No	0.6	–	[101]	
Lifetime	Photograph (RGB)		283–317	Yes	5.14	0.194	[59]	
			273–333	No	4.5	>1	[83]	
			307–313	No	–	0.2	[106]	
Thermochromism	Reflectance spectrum shift	Photograph (RGB)	302–313	Yes	–	0.1	[107]	

^aEstimated value from the data provided by the authors (see Experimental Section for more information); ^bAuthors reported sensitivity (K⁻¹) as not enough data is available to estimate S_r value.

latter, it requires the coupling of a diffraction grating to convert the spectral shift into an angular deviation that can be monitored through the position of the illuminated pixel, quantified from an image. This disturbance is afterward correlated with temperature to characterize the sensor. These examples will be detailed in the following sections.

3.1.1. Intensity-Based Measurement

Surface plasmonic resonance (SPR) sensors are implemented based on the intensity or spectral variation of the input guided signal. The lack of portability and connectivity, relying on expensive equipment, complex optical systems, and accurate alignment of components hamper commercial applications.^[94] Efforts have been made to overcome these difficulties by presenting fiber-optic SPR sensors as an alternative to traditional SPR sensors.^[95] Lu et al. reported a fiber-optic SPR sensor using a smartphone able to monitor the temperature in the range from 303 to 340 K with a sensitivity of $0.0018 \text{ a.u. K}^{-1}$ (estimated $S_r \approx 0.27\% \text{ K}^{-1}$, Table 1 and Experimental Section for details). The sensing system is composed of a side-polished-fiber-based SPR sensor illuminated by the light-emitting diode (LED) flash from one end, and the output signals are recorded and processed by the camera and a designed mobile smartphone base application (App). The sensing method uses two photographs, one from a reference signal and the other from the measured signal and the ratio between the grayscale values from both, that have a linear variation with temperature. This low cost and portable system resolution can challenge spectrometer-based SPR systems resolutions although as with other optical fiber thermometers, it has additional equipment that can be dysfunctional for some applications (Figure 4).^[80]

Fujiwara et al. presented a low-cost kit to transform a smartphone into a sensing platform, exploring different types of sensors

based on multimode fibers. At the optical fiber bending zone, the temperature will affect the refractive index value of the core and cladding through thermo-optic effects, changing the light-guiding conditions. This translates into a variation of the propagated light intensity that can be correlated with temperature by a well-established equation. The intensity temperature dependence results in a thermometer sensitivity of $1.29 \times 10^{-2} \text{ }^\circ\text{C}$ (estimated $S_r \approx 6.74\% \text{ K}^{-1}$, Table 1 and Experimental Section for details) in the 20–120 °C (293–393 K) range.^[79]

3.1.2. Reflectance Spectrum Shift Measurement

Waveguided optical signal temperature sensors can also work based on reflected or transmitted spectrum peak shift. Pan et al. developed a temperature sensor monitored by a smartphone, taking advantage of TiO₂ optical properties. The system scales down the interrogation system used in optical fiber sensors, making it portable and affordable, using a commercially visible transmission diffraction grating (300 grooves mm⁻¹) mounted on the smartphone camera, in which a LED acts as a light source. At the camera and LED, a bifurcated optical fiber with a temperature-sensitive material is attached. The light emitted by the LED travels through the fiber, interacting with TiO₂ thin film, whose refractive index and thickness vary with temperature resulting in a change of the optical path, yielding a shift of the reflected interference spectrum (Figure 5).^[93] This shift is linear in the range from 263 to 453 K with a sensitivity of $0.46 \text{ pixel K}^{-1}$ (estimated $S_r \approx 0.07\% \text{ K}^{-1}$, Table 1 and Experimental Section for details). This system reduces the costs and increases the portability at the expense of having additional apparatus. It illustrates how optical fiber sensors can impact IoT, as they have a simple concept that can be low cost, smart, and incorporated into a sensor network.

From the works described so far, fiber optics sensors are based on the perturbation of the guided light inside the fiber

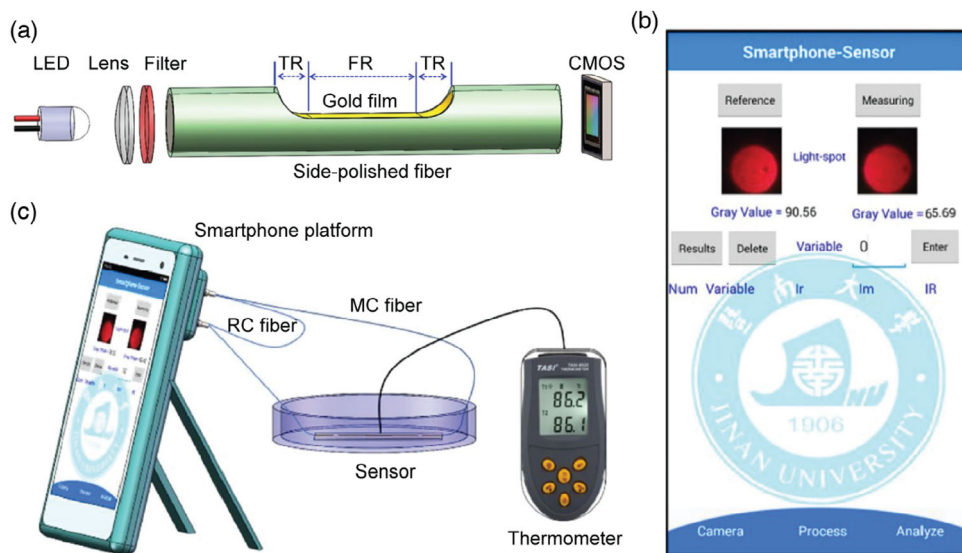


Figure 4. a) Schematic diagram of the SPR-based sensing system. b) Interface of the designed smartphone application. c) Schematic diagrams of the assembled sensing system and the experimental setup. Reproduced under the terms of the CC-BY license.^[80] Copyright 2019, The Authors, published by Optical Society of America.

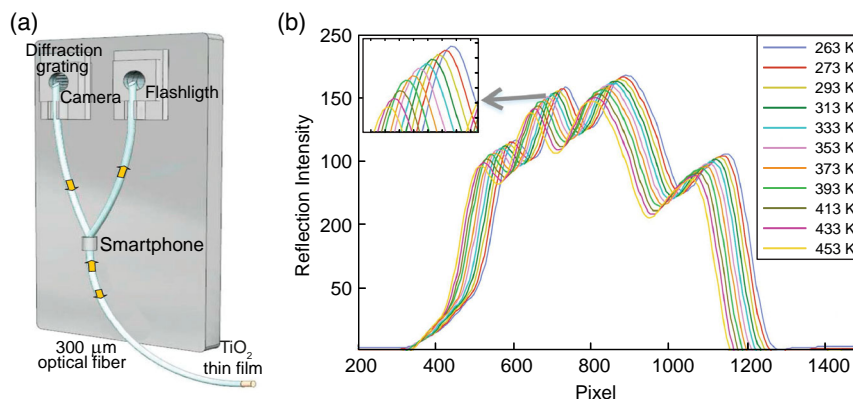


Figure 5. a) Schematic of the temperature sensor based on a smartphone. Note that, the arrows in the original diagram are misplaced as the light should come out from the flashlight and go into the camera. b) Reflectance spectra of the sensor at different temperatures. Reproduced with permission.^[93] Copyright 2018, Elsevier Inc.

(intensity variation and spectral peak shift) due to temperature effects and their analyses can be made using a smartphone without compromising the figures of merit. Nevertheless, we must consider that waveguided sensors are based on optical phenomena that occur inside a waveguide and not due to an intrinsic optical property of the material, as the sensors to be presented in nonguided optical sensors. This can make them more sensitive to external perturbations, as strain, displacement, humidity, or other parameters affecting the light guiding. In some cases, without changing the sensor configuration, they can act as a multiparameter sensor, depending on the characterization made and the calibration to be used. This is exemplified by the work of Markvart et al. that develop a strain sensor based not only on the spectral shift in the guided light created by a fiber Bragg grating using an analysis similar to

the one in Pan et al. but also manage to characterize it as a temperature sensor.^[96]

3.2. Nonguided Optical Signal Temperature Sensors (Cluster II)

Cluster II sensors in IoT include luminescent thermometers, using the lifetime and the variation in the emission intensity as thermometric parameters, and also examples in which the temperature sensing is mediated by the analysis of the reflectance spectrum. The examples that will be discussed exclude measurements requiring the use of a spectrometer and refer to those in which the thermometric parameter can be based on images acquired by a CCD camera. Some of the examples do not include an IoT connection^[84,97] but the methodology is easily transposed to mOptical sensing. As shown in Figure 3a,

the S_m values (solid symbols) compare well with those found for spectrometer-based luminescence thermometry.

3.2.1. Emission Intensity-Based Measurement

Othong et al. developed a dual function sensor based on $\text{Cd}_2(2,5\text{-tpt})(4,5\text{-idc})(\text{H}_2\text{O})_4$ to detect the water percentage and measure the temperature using the emission color dependence in the 303–393 K range. Under 360 nm excitation, it is visible at the naked eye a color shift (≈ 24 nm) from the yellow-green to the green-blue regions, with an estimated $S_r \approx 0.06\% \text{K}^{-1}$ (Table 1 and Section 5 for details). Noticeably, the smartphone was only used to sense the water percentage by the intensity ratio between the R and G coordinates associated with color change. Even though this technique was not transposed to the temperature analyses, one can assume that if it was, a thermometric parameter could have been defined possibly as a ratio between cyan and yellow coordinates (to note that cyan is the complementary color of red, $C = 1 - R$, and yellow the complementary of blue, $Y = 1 - B$) and temperature could have been quantified using a smartphone as they did to the water percentage.^[98]

Another work based on the temperature dependence of the luminescence intensity is presented by Kumbhakar et al. using Mn^{2+} -doped ZnS quantum dots (MZQDs) encapsulated into a polymer thin film, in the 303–418 K range with sensitivity of $= 0.164 \text{K}^{-1}$. The emission spectrum is formed by two well-defined bands at 400 and 595 nm, whose relative intensity depends on the temperature inducing color variation as the temperature increases. This emission color dependence is also detected in the photographic records (RGB coordinates) of the MZQD-based films. The thermometric parameter was set as the difference between the intensity at room temperature and the intensity at the different temperatures. A custom-made App able to capture photography and measure the color intensity was also developed.^[99]

The potential of using a smartphone as a device in temperature sensing as an alternative to other methods was also presented by Lee et al. A polyethylene glycol-functionalized graphene oxide based colorimetric thermosensor using guanine rich DNzyme and peptide nucleic acid assisted by a smartphone was developed creating a colorimetric platform for distinct IoT scenarios (e.g., health diagnostics or food safety). The material changes from transparent to green as the temperature increases in the 277–353 K range. This color change is perceived at the naked eye and was quantified through images taken with a smartphone and an image analyzer software to retrieve the green color coordinate intensity.^[100]

Other examples of intensity-based sensors include ratiometric thermometers. Shi et al., exploit dihydrophenazine-based ratiometric thermometers excited at 365 nm (Table S3 in Supporting Information), over a temperature range 278–408 K, using the spectral emission dependence with temperature quantified by the ratio between the intensities of the orange–red and blue emission bands presenting $S_r = 3.40\% \text{K}^{-1}$ (Table 1). The emission dependence with temperature is visible at the naked eye as the color changes from blue at low temperature (278 K) to orange–red at high temperature (408 K). Although the color quantification was only carried out using spectral data, the broad

color variation in this range of temperatures is remarkable. Such color dependence with temperature could be further explored to develop IoT temperature sensor labels as they can be coated onto any object surface for simple and fast large-area temperature detection. As presented by Ma et al., temperature-sensitive Zn^{2+} and Co^{2+} metal–ligand complexes incorporated into polyethylene glycol (Table S3, Supporting Information) with tunable color were used as a counterfeit label.^[84,97] This work presents a similar idea to that of Shi et al. in which the Zn^{2+} complex (Table S3, Supporting Information) displays a color response with temperature under 365 nm excitation. Using the ratio between the blue and the yellow transitions, the thermometric parameter shifts from the blue to the yellow spectral ranges in the range 298–338 K range excitation and with a $S_r = 2.17\% \text{K}^{-1}$ (Table 1). While both works refer to thermometers with remarkable sensitivities and enormous potential, they lack a direct application into IoT.

Following the same research direction, Piotrowski et al. presented thermochromic luminescent nanomaterials codoped with $\text{Mn}^{4+}/\text{Tb}^{3+}$ (Table S3, Supporting Information) for temperature sensing, presenting a color variation from red to green as the temperature changes from 298 to 425 K, under 266 nm excitation, obtaining a maximum S_r calculated from Commission Internationale d'Éclairage (CIE) 1931 color coordinates of $0.6\% \text{K}^{-1}$ (Table 1). The color variation occurs due to a decrease in the Mn^{4+} -related emission (the red component of the spectra) as the temperature increases, whereas the Tb^{3+} -based emission is independent of the temperature. The relative variation between the Mn^{4+} and Tb^{3+} emission spectra induces a shift in the color from the red to the green spectral regions. Moreover, the emission color temperature dependence was explored a step further, as the color variation was also quantified using photographic records from a digital camera in the RGB color system, complementing the analysis of spectral data to in CIE 1931 color coordinates (Figure 6).^[101] This is a representative example that quantifies emission color through remote captured images even though the full temperature range is very broad and outside the expected working regime for a smartphone. Nonetheless, as luminescence thermometry is a noncontact method, it is feasible to consider the use of a smartphone, illustrating its use for temperature sensing in more extreme scenarios.

Examples in which IoT is explicitly included were presented by us, Ramalho et al. In a step forward, the popularization of luminescence thermometry smart QR codes in IoT,^[102] photographs of QR codes printed using luminescent inks and recorded by a smartphone were used to sense, in real time, the absolute temperature (283–317 K) with a $S_r = 5.14\% \text{K}^{-1}$, and $\partial T = 0.194$ K (Table 1).^[59] An end-to-end process for an optical thermometer for IoT based on smartphone technology and luminescent QR codes was developed by Ramalho et al. It was demonstrated how photographs of QR codes printed using luminescent inks based on organic–inorganic hybrid codoped with europium (Eu^{3+}) and terbium (Tb^{3+}) ions and recorded by a smartphone, could be used to sense, in real time, the absolute temperature (283–317 K) with $S_r = 5.14\% \text{K}^{-1}$ and a resolution of 0.194 K, being the first example of an intramolecular primary thermometer (Figure 7). Processing the material in a form of QR codes gave the opportunity to easily interact with the smartphone, using a custom developed App, providing temperature

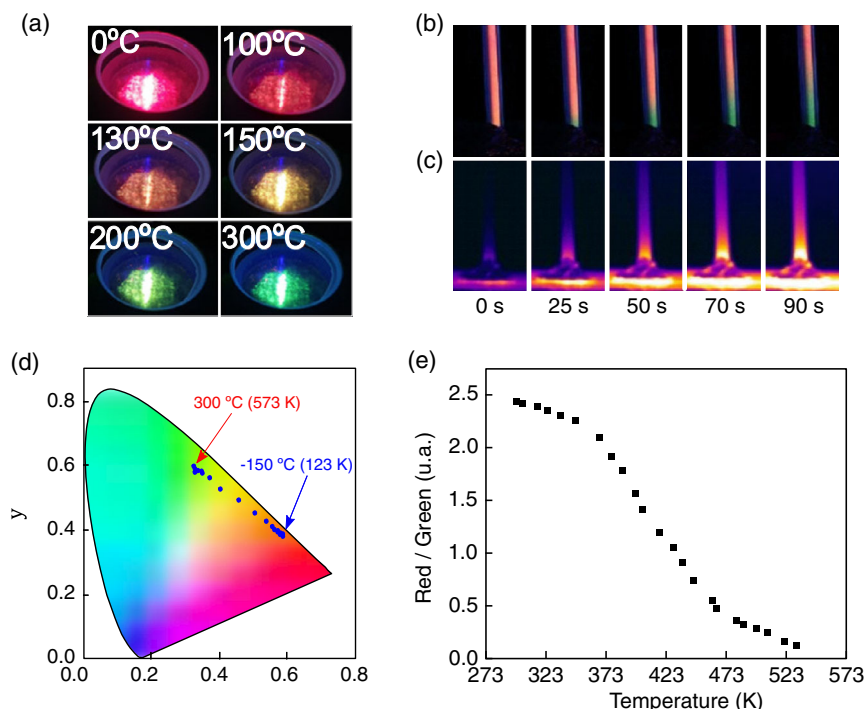


Figure 6. a) Photographs of the SAO:0.1% Mn⁴⁺, 5% Tb³⁺ powder under 266 nm laser illumination at different temperatures. b) Photographs from a digital color camera and c) thermal camera of a quartz tube with SAO:0.1% Mn⁴⁺, 5% Tb³⁺ powder under UV light excitation recorded at different heating exposition times. d) CIE1931 chromaticity diagram for SAO:0.1% Mn⁴⁺, 5% Tb³⁺ powder. e) Ratio of red to green emission intensity channels as a function of temperature controlled using a thermal camera. Reproduced with permission.^[101] Copyright 2020, American Chemical Society.

information in real time, and being able to be inserted into a sensor network.^[59,103]

3.2.2. Reflectance Spectrum Shift Measurement

In the nonguided optical signal thermometers based on the reflectance spectra shift, Choi et al. developed a colorimetry sensor using thin, soft, and skin-compatible microfluidic systems that include networks of microfluidic channels, inlet/outlet ports, microreservoirs, to carry out sweat analyses (pH, temperature, concentrations of chloride, glucose, and lactate) in physiologically relevant ranges from 305 to 310 K with a $\partial T = 0.2$ K (Table 1), **Figure 8.**^[104–106] This optical sensor is based on the reflectance of the material avoiding the need for external excitation, unlike emission-based sensors where external excitation is necessary. These colorimetry sensors performing quantitative analyses for extracting absolute values are affected by the surrounding illumination conditions, requiring a fine-tuned color reference marker to be placed near the measurement site to facilitate the analyses independently from lightning conditions. The authors present a systematic study verifying that proper use of the reference markers can yield accurate color information in a wide range of lighting conditions, proving that this can be a reliable path for other optical temperature sensors to deal with ambient light conditions.

A thermochromic ternary cholesteric liquid crystalline mixture of 40 wt% cholesteryl oleyl carbonate, 40 wt% cholesteryl

nonanoate, and 20 wt% cholesteryl 2,4-dichlorobenzoate encapsulated by a film of polyester (25 μm thick, Table S3 in Supporting Information) was used. The film presents a broad color variation, red (305 K), green (306 K), and blue (307 K) ending in the absence of color at 310 K, quantified via digital images using the RGB color space. The entire process could have been carried out entirely with a smartphone, whose capability to analyze the color in a small area of an image is easily attained with a commercial App, especially with a palette having such different colors leaving room for further improvement and, once again, opening the door for IoT, as evaluation can be made in real time, inside a physiological temperature range with a smartphone.

The use of thermochromic liquid crystals was also explored by Moreddu et al. embedding them into contact lenses to measure corneal temperature based on the reflectance spectra shift. The liquid crystal was obtained by the mixture of cholesteryl oleyl carbonate, cholesteryl nonanoate, and cholesteryl benzoate (wt%, 0.35:0.55:0.10, respectively) that when melted together retains its unique chemical properties. There is a shift in the reflected wavelength from 738 to 473 nm (red to blue in the visible spectrum) in a small temperature variation of 11 K (302–313 K) having an average $\partial T = 0.3$ K (Table 1). The color quantification was made using a commercial App, returning RGB values for each image afterward correlated with temperature. A color shift of this magnitude can be easily accessed by an unchanged smartphone, from image acquisition and processing to image analyses. These contact lenses that can measure ocular surface temperature

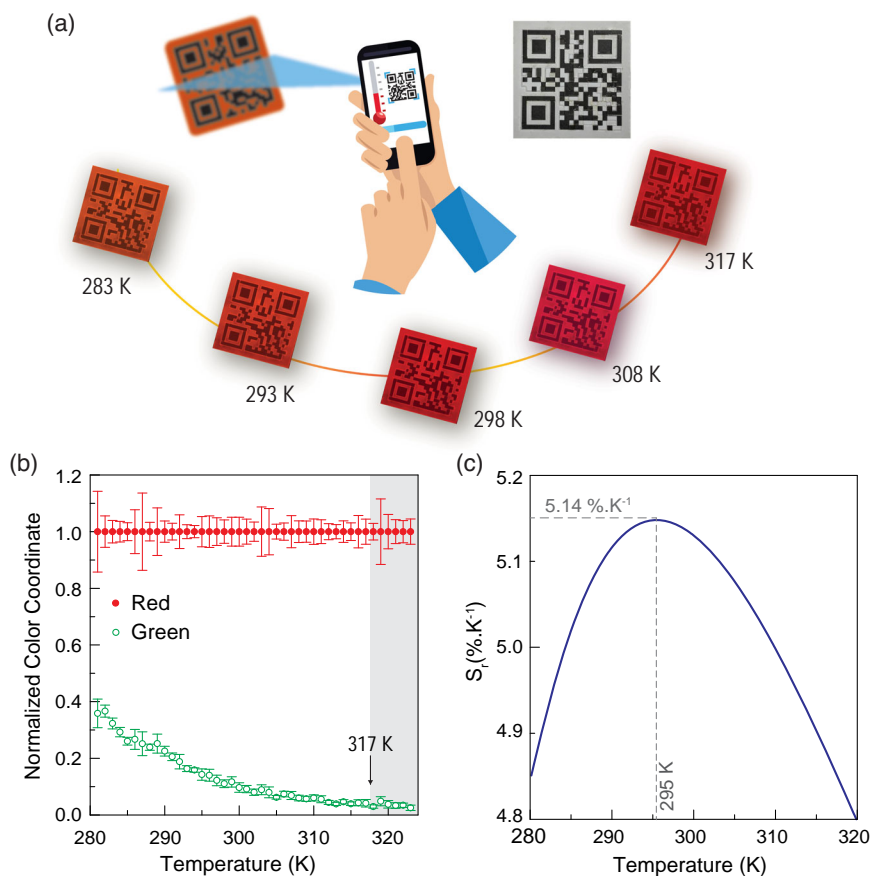


Figure 7. a) Schematic representation of the temperature sensing and message decoding using a smartphone to read luminescent QR codes. b) Normalized red and green color coordinates variation with temperature (283–323 K) calculated from the photographic records of the luminescent QR code at different temperatures and c) relative thermal sensitivity. Reproduced with permission.^[59] Copyright 2019, Wiley-VCH.

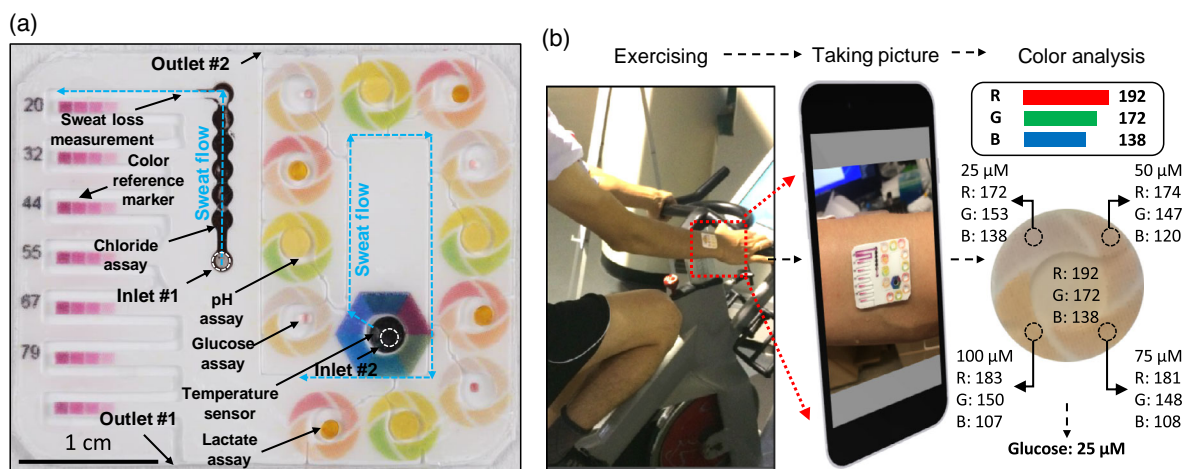


Figure 8. a) Top view illustration of microfluidic channels filled with blue-dyed water. b) Procedure for collecting sweat samples and color analysis of digital images of the device. Reproduced with permission.^[107] Copyright 2019, American Chemical Society.

in real time, which is desirable for point-of-care diagnostics and disease monitoring.^[107] In a later article by the same author, where the same idea was exploited to sense other parameters, a custom

App was presented, allowing to store data and create a personal record that could be sent to a healthcare provider, becoming a part of IoT. The potential of this technology, if available for a common

person to monitor themselves exchanging data or having their data analyses in real time (telemedicine), could help target early-stage diagnosis and/or monitor ocular infections.^[108]

3.2.3. Lifetime-Based Measurement

Recently, Katumo et al. proceed with a new trend in the literature that is visible across fields. The idea is to transform techniques that are only accessible in controlled laboratory conditions with specific equipment into an affordable and inexpensive format to allow more general applications. They exploit luminescence thermometry using a smartphone as a tool to quantify temperature, as a cheap alternative to thermal cameras that are usually very expensive. Moreover, thermal cameras also display the disadvantages of lacking good spatial resolution, the calibration, and temperature measurements are dependent on the object and the knowledge of their properties (e.g., emissivity).^[24] Temperature is measured using a phosphor whose lifetime is temperature-dependent and is also long enough to be recorded by a 30 fps CCD camera (≈ 1 frame every 30 ms). The measurement requires the recording of a video with a smartphone and the subsequent analyses are carried out in a computer that evaluates the intensity variation of the red channel. This evaluation was made by adding every coordinate in a region of interest and a decrease in the emission intensity of the phosphor was observed in every consecutive frame. The performance of the thermometer reached a $S_r = 4.5\%K^{-1}$ (Table 1) at 273 K and $\partial T > 1$ K for temperature below 300 K increasing to $\partial T = 2.5$ K at around 333 K in the temperature range from 273 to 333 K using 375 nm excitation. This approach includes a smartphone and although the analyses and excitation are externally provided, it is an important step toward mOptical sensing for IoT, as smartphones are widely available and easily accessible equipment for science and engineering to use.^[83]

3.3. Discussion

The end-to-end operation idea applied by Ramalho et al., Moreddu et al., and more recently by Kumbhakar et al. could be easily translated to other works, either the ones using luminescence or thermochromism, using smartphones to quantify the temperature without the necessity of having additional equipment, while the works of Pan et al., Lu et al., and Fujiwara et al. in the field of waveguided optical signal thermometers, proved that is possible to reduce the costs while maintaining the main features and figures of merit for that type of sense.

An overview of the key parameters and figures of merit is shown in Table 1 comparing both waveguided and nonguided optical signal sensors (see Experimental Section for the mathematical definition). When possible, the relative sensitivity was also calculated, as defined by Wade et al. and proposed as a figure of merit for luminescence thermometry by Brites et al., as it appears as a definition shared by both fields, so that a comparison is possible.^[35,109] From Table 1, it is possible to infer that the main input for all systems is photographic records used to analyze the intensity of the pixels to calculate an intensity ratio, a shift in the reflectance spectrum, or a lifetime value. Those parameters are traditionally calculated from data acquired with

expensive laboratory equipment, and these works were able to do it with inexpensive and easily accessible equipment. The figure-of-merit that enables performance comparison between waveguided and nonguided optical signal temperature sensors is relative sensitivity (see Experimental Section for more information), which is independent of the thermometric parameter. It is also noticeable from Table 1 that, similarly to luminescence thermometry, the radiometric approach is the most popular having an overall maximum relative sensitivity value and when comparing the physical mechanisms involved, the luminescence-based thermometers present, in general, higher values (around one order of magnitude) than their counterparts.

It is interesting that the aforementioned examples that combine emission and a smartphone, or a digital camera, adapt and develop the methodologies typically used in the luminescence thermometry fields, Figure 2. Traditionally, the measurement of those parameters (and consequently the temperature quantification) requires the need for a spectrometer or an optical interrogator to acquire the optical input (e.g., spectrum or decay curves). Another aspect of thermometry under study is sensing using smartphones.^[59] In a step forward toward the popularization of luminescence thermometry, photographs of luminescent materials recorded by a smartphone could be used to sense, in real-time, the absolute temperature. The decoding tool and the temperature sensing require only a CCD, thus smartphones and closed-circuit television, also known as video surveillance, may be used in their original configuration to sense temperature forming a distributed network of thermal sensors. This sensing network will be based on simple, widely available, and unchanged smartphone or digital cameras, proving that the well-established methods can be used by acquiring an image not compromising the result, and represents an important advance in the field of optical temperature sensors. The mOptical sensing requires the development of phosphors with improved optical features suitable to operate in combination with a smartphone (or similar devices in the future), acting as a sensing probe (e.g., increasing the emission color change or the lifetime value or broadening the temperature sensing range). In parallel, the excitation/illumination source is a challenge requiring high-quality LEDs to be used externally or to be incorporated into the smartphone. Despite the high processing capacity of the current smartphones, an optical to the electronic signal converter with a quality equivalent to traditional equipment still fails to perform as high quality and reliable excitation/illumination source. This need will benefit from the noticeable enhancement of the external quantum efficiency of compact and higher output near-UV-emitting LED pushing and suit well engineering needs in a bordering field.^[110]

4. Conclusion

In this work, a literature survey was carried out to outline the recent developments of optical temperature sensors. In this short overview enclosing different optical technologies with potential applications in future smart infrastructures, namely IoT, we observed that keywords representing indexing terms typically associated with waveguided and nonguided optical sensors tend to cluster in two distinct groups. The results presented so far

prevent us to infer whether any of them will be predominant in IoT and mOptical as the examples of optical temperature sensors for IoT reported so far are scarce. Both waveguided optical signal and nonguided optical signal thermometers reveal serious arguments to be an alternative to electronic thermometers, which so far are the dominant technology in the field of mOptical sensing and are already moving toward IoT.

Waveguided optical signals systems have the advantage of including several types of sensors with high sensitivity, that can be spread across a vast distance, but they are mainly stationary because they require the attachment of the optical fiber to the detection and the illumination device as an extra piece of equipment. For non-guided optical signal thermometers breakthrough into IoT and our daily life, smartphone usage seems to be the obvious route, as this technology is an on-growing trend in many different sensing areas (not yet in thermometry). Their increased use is due to their widespread availability and (more important) to their ability to perform the transition from optics to electronics which is, until now, one key base topic. This will allow nonguided optical signal thermometry to be part of a large complex sensors network, leaving specific equipment for specific niche applications (e.g., e-medicine).

From the examples here, it is clear that progress has been made in introducing mOptical sensors into IoT, even though at this stage none of the works is robust enough for a real scenario application. The key point is to look at all strengths and the common aspects between works and envision a temperature sensor that combines them. The strengths are a broad color variation to reduce readout errors, a broad temperature range to maximize the number of applications, being able to carry out without any prior calibration and the ability to perform without any external illumination source in addition to the smartphone LED. However, the common points are the use of a smartphone (mobile device or camera) and the temperature quantification using a photograph. Having a temperature-sensing probe with those features working in a combination with a good design and user-friendly App able to take care of all the data collection (image or live video) and, most important, all the data processing and temperature quantification would create a robust thermometer capable to be operated by both individuals and industries in a multitude of different areas of expertise from industry 4.0, healthcare 4.0 to smart cities.

Challenges for the future must encompass distinct fields of science, either centered in materials science with the development of new materials increasingly suitable for mOptical sensing and in computer science and engineering developing new and specific software (mobile applications) to work with today's widely available hardware (smartphone), toward the collection and analyses of information that the materials provide, either to sense temperature or any other physical or chemical parameter. Only with the merge of the two areas toward the same objective will be possible to keep on moving forward, creating new alternatives to traditional methods and seizing the opportunities offered by today's technology. In conclusion, such advances in photonics research, foresee that currently available and emerging optical technologies for sensing will contribute to a large number of globally connected IoT devices and systems with relevant societal impact.

5. Experimental Section

Bibliographic Survey: To have a broad view of the published literature, a survey of the field of optical temperature sensors was made using CitNetExplorer and VOSviewer tools and a sample data consisting of the information from 11 692 published articles, letters, reviews, and books from the principal Web of Knowledge collection containing the following citation indexes: SCI-EXPANDED, SSCI, A&HCI, CPCI-S, CPCI-SSH, ESCI, CCR-EXPANDED, and IC, using the search terms in all fields: (thermosens* OR "temperature monitoring" OR "temperature sens*" OR thermometer* OR "temperature-sens*") AND (optic* OR color OR colour OR colorimet* OR reflectance OR transmittance OR luminesce* OR emission) in the period from 1999 to 2021, accessed on February 4, 2021.

From each article, information was obtained such as authors' names, affiliation and funding entity, the document title, keywords, abstract, and reference list, the publication citations and date and the journal information, allowing to analyze the field in a multitude of parameters. We analyzed the field by creating a map based on text data (Figure 1), which means that the abstracts and titles were scanned for terms or verified whether a term is present or not (binary counting) and if it has a link with some other term (both appear in the same document). If the term appeared in a document, it is counted as one occurrence and if two terms appear together in the same document (co-occurrence), a link is created between them. The number of occurrences a term was represented by the size of its circle, and the number of co-occurrences between two terms was represented by the width of the line connecting them. Also, the proximity of terms in the map was representative of how closely related they were, despite having a co-occurrence or not, even though in some cases, a term was linked with many others that were not related it can appear further away, being placed in the middle of all his connections. There was also the aggregation of terms that were homonym but had different interpretations depending on the field. An example of this is the terms marked in blue in Figure 1, that despite being closely related to all others (having many strong connections), they do not appear close to either, being placed in the middle. Based on these connections, it was possible to defined clusters and as shown in Figure 1, these clusters contained indexing terms that are representative of different fields of study. The analyses also allowed us to have a clear view of the field evolution over the years and what elements were trending.^[111,112]

From these articles, we refined the search to include only smartphone-related works, reviewing these examples and other works directly related to those articles (citing or citation), to analyze the evolution of optical temperature sensors for mOptical sensing in the context of the IoT.

Figures of Merit for Optical Sensing: To compare the performance of the thermometers, the relative thermal sensitivity (S_r , %K⁻¹) was calculated (marked values in Table 1) using the temperature thermometric parameter Δ and $\delta\Delta/\delta T$, the derivative of the Δ parameter to temperature (T).^[52,109]

In the work of Pan et al.,^[93] the thermometric parameter was defined as the peak position, having a variation from around pixel 732 to 644 in the temperature range from 263 to 453 K, given by the estimated equation

$$\Delta(T) = -46.32 \times 10^{-2} T + 72.73 \times 10 \quad (4)$$

The $\delta\Delta/\delta T = 46.32 \times 10^{-2}$ and divided by the minimum value of Δ (644) to obtain gives the maximum $S_r \approx 0.07\%K^{-1}$.

For the work of Lu et al.,^[80] the thermometric parameter was defined as the relative grey value, that had a variation from 73.48×10^{-2} to 66.28×10^{-2} , in the temperature range from 30 °C (303 K) to 70 °C (340 K) given by the equation

$$\Delta(T) = -1.80 \times 10^{-3} T + 78.88 \times 10^{-2} \quad (5)$$

The $\delta\Delta/\delta T = 1.80 \times 10^{-3}$ and divided by the minimum value of Δ (66.28×10^{-2}) to obtain gives the maximum $S_r \approx 0.27\%K^{-1}$.

In the work of Fujiwara et al.,^[79] the thermometric parameter was defined as the intensity value, that had a variation from 1.89×10^{-2} to 89.37×10^{-2} , in the temperature range from 20 °C (293 K) to 120 °C (393 K) given by the equation

$$\Delta(T) = 8.17 \times 10^{-5} T^2 - 2.69 \times 10^{-3} T + 0.04 \quad (6)$$

The $\delta\Delta/\delta T = 16.34 \times 10^{-3} T - 2.69 \times 10^{-3}$ and divided by $\Delta(T)$ gave the maximum $S_r \approx 6.74\%K^{-1}$.

For the work of Othong et al.,^[98] the thermometric parameter was defined as the emission peak shift, that had a variation from ≈ 495 to 522 , in the temperature range from $30^\circ C$ ($303 K$) to $120^\circ C$ ($393 K$) given by the equation

$$\Delta(T) = -0.309 T + 523.3 \quad (7)$$

The $\delta\Delta/\delta T = 0.309$ and divided by the minimum value of $\Delta(495)$ to obtain gives the maximum $S_r \approx 0.06\%K^{-1}$.

Supporting Information

Supporting Information is available from the Wiley Online Library or from the author.

Acknowledgements

This work was developed within the scope of the project CICECO-Aveiro Institute of Materials (UIDB/50011/2020 & UIDP/50011/2020), Instituto de Telecomunicações (UIDB/EEA/50008/2020), and WINLEDs (POCI-01-0145-FEDER-030351) and Graphsense (POCI-01-0145-FEDER-032072) projects financed by national funds through the FCT/MEC and when appropriate cofinanced by FEDER under the PT2020 Partnership through European Regional Development Fund in the frame of Operational Competitiveness and Internationalization Programme.

Conflict of Interest

The authors declare no conflict of interest.

Keywords

internet of things, luminescence, mobile optical sensing, sensors, temperature

Received: December 30, 2020

Revised: February 17, 2021

Published online: May 6, 2021

- [1] L. Atzori, A. Iera, G. Morabito, *Comput. Networks* **2010**, *54*, 2787.
- [2] J. Gubbi, R. Buyya, S. Marusic, M. Palaniswami, *Future Gener. Comput. Syst.* **2013**, *29*, 1645.
- [3] A. Al-Fuqaha, M. Guizani, M. Mohammadi, M. Aledhari, M. Ayyash, *IEEE Commun. Surv. Tutorials* **2015**, *17*, 2347.
- [4] I. Ud Din, M. Guizani, S. Hassan, B. S. Kim, M. Khurram Khan, M. Atiqzaman, S. H. Ahmed, *IEEE Access* **2019**, *7*, 7606.
- [5] E. Sisinni, A. Saifullah, S. Han, U. Jennehag, M. Gidlund, *IEEE Trans. Ind. Informatics* **2018**, *14*, 4724.
- [6] G. Aceto, V. Persico, A. Pescapé, *J. Ind. Inf. Integr.* **2020**, *18*, 100129.
- [7] A. Zanella, N. Bui, A. Castellani, L. Vangelista, M. Zorzi, *IEEE Internet Things J.* **2014**, *1*, 22.
- [8] N. Abbas, Y. Zhang, A. Taherkordi, T. Skeie, *IEEE Internet Things J.* **2018**, *5*, 450.
- [9] Y. Liu, M. Peng, G. Shou, Y. Chen, S. Chen, *IEEE Internet Things J.* **2020**, *7*, 6722.
- [10] S. M. Tahsien, H. Karimipour, P. Spachos, *J. Netw. Comput. Appl.* **2020**, *161*, 102630.
- [11] S. K. Singh, S. Rathore, J. H. Park, *Future Gener. Comput. Syst.* **2020**, *110*, 721.
- [12] J. Qiu, Z. Tian, C. Du, Q. Zuo, S. Su, B. Fang, *IIE Internet Things J.* **2020**, *7*, 4682.
- [13] K. Shafique, B. A. Khawaja, F. Sabir, S. Qazi, M. Mustaqim, *IEEE Access* **2020**, *8*, 23022.
- [14] C. Wu, A. C. Wang, W. Ding, H. Guo, Z. L. Wang, *Adv. Energy Mater.* **2019**, *9*, 1802906.
- [15] A. Nozariasbmarz, H. Collins, K. Dsouza, M. H. Polash, M. Hosseini, M. Hyland, J. Liu, A. Malhotra, F. M. Ortiz, F. Mohaddes, V. P. Ramesh, Y. Sargolzaeival, N. Snouwaert, M. C. Özturk, D. Vashae, *Appl. Energy* **2020**, *258*, 114069.
- [16] N. H. Motlagh, M. Mohammadrezaei, J. Hunt, B. Zakeri, *Energies* **2020**, *13*, 494.
- [17] G. Chen, Y. Li, M. Bick, J. Chen, *Chem. Rev.* **2020**, *120*, 3668.
- [18] J. Meng, Z. Li, *Adv. Mater.* **2020**, *32*, 2000130.
- [19] F. Mao, K. Khamis, J. Clark, S. Krause, W. Buytaert, B. F. Ochoa-Tocachi, D. M. Hannah, *Environ. Sci. Technol.* **2020**, *54*, 9145.
- [20] M. Faheem, S. B. H. Shah, R. A. Butt, B. Raza, M. Anwar, M. W. Ashraf, M. A. Ngadi, V. C. Gungor, *Comput. Sci. Rev.* **2018**, *30*, 1.
- [21] L. M. Ang, K. P. Seng, A. M. Zungeru, G. K. Ijamaru, *IEEE Internet Things J.* **2017**, *4*, 1259.
- [22] T. Qiu, N. Chen, K. Li, M. Atiqzaman, W. Zhao, *IEEE Commun. Surv. Tutorials* **2018**, *20*, 2011.
- [23] L. Russell, R. Goubran, F. Kwamena, F. Knoefel, *IEEE Internet Things J.* **2018**, *5*, 4454.
- [24] X. D. Wang, O. S. Wolfbeis, R. J. Meier, *Chem. Soc. Rev.* **2013**, *42*, 7834.
- [25] X. D. Wang, O. S. Wolfbeis, *Anal. Chem.* **2016**, *88*, 203.
- [26] C. D. S. Brites, S. Balabhadra, L. D. Carlos, *Adv. Opt. Mater.* **2019**, *7*, 1801239.
- [27] J. Albert, L. Y. Shao, C. Caucheteur, *Laser Photonics Rev.* **2013**, *7*, 83.
- [28] R. A. S. Ferreira, C. D. S. Brites, C. M. S. Vicente, P. P. Lima, A. R. N. Bastos, P. G. Marques, M. Hiltunen, L. D. L. D. Carlos, P. S. André, *Nano Lett.* **2013**, *1035*, 1027.
- [29] P. Lu, N. Lalam, M. Badar, B. Liu, B. T. Chorpening, M. P. Buric, P. R. Ohodnicki, *Appl. Phys. Rev.* **2019**, *6*, 041302.
- [30] B. H. Lee, Y. H. Kim, K. S. Park, J. B. Eom, M. J. Kim, B. S. Rho, H. Y. Choi, *Sensors* **2012**, *12*, 2467.
- [31] P. Roriz, S. Silva, O. Frazão, S. Novais, *Sensors* **2020**, *20*, 2113.
- [32] R. J. Mears, L. Reekie, I. M. Jauncey, D. N. Payne, R. J. Mears, *Electron. Lett.* **1987**, *23*, 1026.
- [33] D. J. J. Hu, H. P. Ho, *Adv. Opt. Photonics* **2017**, *9*, 257.
- [34] Y. Zhao, X. G. Li, X. Zhou, Y. N. Zhang, *Sens. Actuators B Chem.* **2016**, *231*, 324.
- [35] C. D. S. Brites, P. P. Lima, N. J. O. Silva, A. Millán, V. S. Amaral, F. Palacio, L. D. Carlos, *Nanoscale* **2012**, *4*, 4799.
- [36] D. Jaque, F. Vetrone, *Nanoscale* **2012**, *4*, 4301.
- [37] M. D. Dramićanin, *J. Appl. Phys.* **2020**, *128*, 040902.
- [38] J. Zhou, B. del Rosal, D. Jaque, S. Uchiyama, D. Jin, *Nat. Methods* **2020**, *17*, 967.
- [39] H. Suo, X. Zhao, Z. Zhang, Y. Wang, J. Sun, M. Jin, C. Guo, *Laser Photonics Rev.* **2020**, *2000319*, 1.
- [40] M. Suta, A. Meijerink, *Adv. Theory Simulations* **2020**, *2000176*, 1.
- [41] M. Jia, Z. Sun, M. Zhang, H. Xu, Z. Fu, *Nanoscale* **2020**, *12*, 20776.
- [42] A. Bednarkiewicz, L. Marciniak, L. D. Carlos, D. Jaque, *Nanoscale* **2020**, *12*, 14405.
- [43] E. D. Martínez, C. D. S. Brites, L. D. Carlos, A. F. García-Flores, R. R. Urbano, C. Rettori, *Adv. Funct. Mater.* **2019**, *29*, 1807758.
- [44] L. Marciniak, K. Prorok, L. Francés-Soriano, J. Pérez-Prieto, A. Bednarkiewicz, *Nanoscale* **2016**, *8*, 5037.
- [45] C. D. S. Brites, X. Xie, M. L. Debasu, X. Qin, R. Chen, W. Huang, J. Rocha, X. Liu, L. D. Carlos, *Nat. Nanotechnol.* **2016**, *11*, 851.

- [46] A. Skripka, A. Benayas, R. Marin, P. Canton, E. Hemmer, F. Vetrone, *Nanoscale* **2017**, 9, 3079.
- [47] R. G. Geitenbeek, H. W. De Wijn, A. Meijerink, *Phys. Rev. Appl.* **2018**, 10, 1.
- [48] M. Dramićanin, *Luminescence Thermometry: Methods, Materials and Applications*, Woodhead Publishing, **2018**.
- [49] A. R. Zanatta, D. Scoca, F. Alvarez, *Sci. Rep.* **2017**, 7, 1.
- [50] M. G. Lahoud, R. C. G. Frem, D. A. Gálico, G. Bannach, M. M. Nolasco, R. A. S. Ferreira, L. D. Carlos, *J. Lumin.* **2016**, 170, 357.
- [51] O. A. Savchuk, O. F. Silvestre, R. M. R. Adão, J. B. Nieder, *Sci. Rep.* **2019**, 9, 7535.
- [52] C. D. S. Brites, A. Millán, L. D. Carlos, in *Handbook on the Physics and Chemistry of Rare Earths* (Eds: J.-C. Bünzli, V. K. Pecharsky), Elsevier **2016**, pp. 339–427.
- [53] A. M. P. Botas, C. D. S. Brites, J. Wu, U. Kortshagen, R. N. Pereira, L. D. Carlos, R. A. S. Ferreira, *Part. Part. Syst. Charact.* **2016**, 33, 740.
- [54] L. Labrador-Páez, M. Pedroni, A. Speghini, J. García-Solé, P. Haro-González, D. Jaque, *Nanoscale* **2018**, 10, 22319.
- [55] M. Suta, Ž. Antić, V. Đorđević, S. Kuzman, M. D. Dramićanin, A. Meijerink, *Nanomaterials* **2020**, 10, 543.
- [56] Y. Shen, J. Lifante, N. Fernández, D. Jaque, E. Ximendes, *ACS Nano* **2020**, 14, 4122.
- [57] X. Qiu, Q. Zhou, X. Zhu, Z. Wu, W. Feng, F. Li, *Nat. Commun.* **2020**, 11, 1.
- [58] J. C. Martins, A. R. N. Bastos, R. A. S. Ferreira, X. Wang, G. Chen, L. D. Carlos, *Adv. Photonics Res.* **2021**, 2000169.
- [59] J. F. C. B. Ramalho, S. F. H. Correia, L. Fu, L. L. F. António, C. D. S. Brites, P. S. André, R. A. S. Ferreira, L. D. Carlos, *Adv. Sci.* **2019**, 6, 1900950.
- [60] C. D. S. Brites, E. D. Martínez, R. R. Urbano, C. Rettori, L. D. Carlos, *Front. Chem.* **2019**, 7, 267.
- [61] A. S. Souza, L. A. O. Nunes, I. G. N. Silva, F. A. M. Oliveira, L. L. Da Luz, H. F. Brito, M. C. F. C. Felinto, R. A. S. Ferreira, S. A. Júnior, L. D. Carlos, O. L. Malta, *Nanoscale* **2016**, 8, 5327.
- [62] S. Balabhadra, M. L. Debasu, C. D. S. Brites, R. A. S. Ferreira, L. D. Carlos, *J. Phys. Chem. C* **2017**, 121, 13962.
- [63] F. J. Caixeta, A. R. N. Bastos, A. M. P. Botas, L. S. Rosa, V. S. Souza, F. H. Borges, A. N. C. Neto, A. Ferrier, P. Goldner, L. D. Carlos, R. R. Gonçalves, R. A. S. Ferreira, *J. Phys. Chem. C* **2020**, 124, 19892.
- [64] M. Back, E. Casagrande, C. A. Brondin, E. Ambrosi, D. Cristofori, J. Ueda, S. Tanabe, E. Trave, P. Riello, *ACS Appl. Nano Mater.* **2020**, 3, 2594.
- [65] D. Pugh-Thomas, B. M. Walsh, M. C. Gupta, *Nanotechnology* **2011**, 22, 185503.
- [66] A. Cadiou, C. D. S. Brites, P. M. F. J. Costa, R. A. S. Ferreira, L. D. Carlos, *ACS Nano* **2013**, 7, 7213.
- [67] M. L. Debasu, D. Ananias, I. Pastoriza-Santos, L. M. Liz-Marzán, J. Rocha, L. D. Carlos, *Adv. Mater.* **2013**, 25, 4868.
- [68] T. Wang, P. Li, H. Li, *ACS Appl. Mater. Interfaces* **2014**, 6, 12915.
- [69] S. Zheng, W. Chen, D. Tan, J. Zhou, Q. Guo, W. Jiang, C. Xu, X. Liu, J. Qiu, *Nanoscale* **2014**, 6, 5675.
- [70] Y. Zhou, B. Yan, F. Lei, *Chem. Commun.* **2014**, 50, 15235.
- [71] S. Balabhadra, M. L. Debasu, C. D. S. Brites, L. A. O. Nunes, O. L. Malta, J. Rocha, M. Bettinelli, L. D. Carlos, *Nanoscale* **2015**, 7, 17261.
- [72] R. Piñol, C. D. S. Brites, R. Bustamante, A. Martínez, N. J. O. Silva, J. L. Murillo, R. Cases, J. Carrey, C. Estepa, C. Sosa, F. Palacio, L. D. Carlos, A. Millán, *ACS Nano* **2015**, 9, 3134.
- [73] Y. Cui, B. Li, H. He, W. Zhou, B. Chen, G. Qian, *Acc. Chem. Res.* **2016**, 49, 483.
- [74] M. Rodrigues, R. Piñol, G. Antorrena, C. D. S. Brites, N. J. O. Silva, J. L. Murillo, R. Cases, I. Díez, F. Palacio, N. Torras, J. A. Plaza, L. Pérez-García, L. D. Carlos, A. Millán, *Adv. Funct. Mater.* **2016**, 26, 200.
- [75] C. D. S. Brites, M. C. Furtos, P. C. Angelomé, E. D. Martínez, P. P. Lima, G. J. A. A. Soler-Illia, L. D. Carlos, *Nano Lett.* **2017**, 17, 4746.
- [76] K. Nigoghossian, Y. Messaddeq, D. Boudreau, S. J. L. Ribeiro, *ACS Omega* **2017**, 2, 2065.
- [77] O. A. Savchuk, J. J. Carvajal, C. D. S. Brites, L. D. Carlos, M. Aguiló, F. Diaz, *Nanoscale* **2018**, 10, 6602.
- [78] A. R. N. Bastos, C. D. S. Brites, P. A. Rojas-Gutierrez, C. DeWolf, R. A. S. Ferreira, J. A. Capobianco, L. D. Carlos, *Adv. Funct. Mater.* **2019**, 29, 1905474.
- [79] E. Fujiwara, P. L. Machado, T. C. D. Oliveira, M. C. P. Soares, T. D. Cabral, C. M. B. Cordeiro, *Sbftot. Int. Opt. Photonics Conf.* **2019**, <https://doi.org/10.1109/SBFoton-IOPC.2019.8910250>.
- [80] L. Lu, Z. Jiang, Y. Hu, H. Zhou, G. Liu, Y. Chen, Y. Luo, Z. Chen, *Opt. Express* **2019**, 27, 25420.
- [81] Y. Chen, J. He, X. Zhang, M. Rong, Z. Xia, J. Wang, Z. Q. Liu, *Inorg. Chem.* **2020**, 59, 1383.
- [82] M. Jia, Z. Sun, H. Xu, X. Jin, Z. Lv, T. Sheng, Z. Fu, *J. Mater. Chem. C* **2020**, 8, 15603.
- [83] N. Katumo, G. Gao, F. Laufer, B. S. Richards, I. A. Howard, *Adv. Opt. Mater.* **2020**, 8, 2000507.
- [84] Y. Ma, Y. Dong, S. Liu, P. She, J. Lu, S. Liu, W. Huang, Q. Zhao, *Adv. Opt. Mater.* **2020**, 8, 1901687.
- [85] E. V. Salerno, J. Zeler, S. V. Eliseeva, M. A. Hernández-Rodríguez, A. N. Carneiro Neto, S. Petoud, V. L. Pecoraro, L. D. Carlos, *Chem. Eur. J.* **2020**, 26, 13792.
- [86] O. Savchuk, J. J. C. Marti, C. Cascales, P. Haro-Gonzalez, F. Sanz-Rodríguez, M. Aguiló, F. Diaz, *Nanomaterials* **2020**, 10, 993.
- [87] M. Sójka, C. D. S. Brites, L. D. Carlos, E. Zych, *J. Mater. Chem. C* **2020**, 8, 10086.
- [88] S. Wang, S. Ma, J. Wu, Z. Ye, X. Cheng, *Chem. Eng. J.* **2020**, 393, 124564.
- [89] Z. Zhang, H. Suo, X. Zhao, C. Guo, *Photon. Res.* **2020**, 8, 32.
- [90] D. Zhang, Q. Liu, *Biosens. Bioelectron.* **2016**, 75, 273.
- [91] S. Kanchi, M. I. Sabela, P. S. Mdululi, Inamuddin, K. Bisetty, *Biosens. Bioelectron.* **2018**, 102, 136.
- [92] K. E. McCracken, J. Y. Yoon, *Anal. Methods* **2016**, 8, 6591.
- [93] T. Pan, W. Cao, M. Wang, *Opt. Fiber Technol.* **2018**, 45, 359.
- [94] Y. Liu, Q. Liu, S. Chen, F. Cheng, H. Wang, W. Peng, *Sci. Rep.* **2015**, 5, 12864.
- [95] S. S. Hinman, K. S. McKeating, Q. Cheng, *Anal. Chem.* **2018**, 90, 19.
- [96] A. A. Markvart, L. B. Liokumovich, I. O. Medvedev, N. A. Ushakov, *J. Light. Technol.* **2021**, 39, 282.
- [97] L. Shi, W. Song, C. Lian, W. Chen, J. Mei, J. Su, H. Liu, H. Tian, *Adv. Opt. Mater.* **2018**, 6, 1800190.
- [98] J. Othong, J. Boonmak, F. Kielar, S. Youngme, *ACS Appl. Mater. Interfaces* **2020**, 12, 41776.
- [99] P. Kumbhakar, A. R. Karmakar, G. P. Das, J. Chakraborty, C. S. Tiwary, P. Kumbhakar, *Nanoscale* **2021**, 13, 2946.
- [100] J. Lee, W. K. Kim, *J. Ind. Eng. Chem.* **2021**, 94, 457.
- [101] W. Piotrowski, K. Trejgis, K. Maciejewska, K. Ledwa, B. Fond, L. Marciniak, *ACS Appl. Mater. Interfaces* **2020**, 12, 44039.
- [102] J. F. C. B. Ramalho, S. F. H. Correia, L. Fu, L. M. S. Dias, P. Adão, P. Mateus, R. A. S. Ferreira, P. S. André, *npj Flex. Electron.* **2020**, 4, 11.
- [103] J. F. C. B. Ramalho, L. C. F. António, S. F. H. Correia, L. S. Fu, A. S. Pinho, C. D. S. Brites, L. D. Carlos, P. S. André, R. A. S. Ferreira, *Opt. Laser Technol.* **2018**, 101, 304.
- [104] J. Choi, Y. Xue, W. Xia, T. R. Ray, J. T. Reeder, A. J. Bandodkar, D. Kang, S. Xu, Y. Huang, J. A. Rogers, *Lab Chip* **2017**, 17, 2572.
- [105] J. Choi, D. Kang, S. Han, S. B. Kim, J. A. Rogers, *Adv. Healthc. Mater.* **2017**, 6, 1601355.
- [106] J. Choi, A. J. Bandodkar, J. T. Reeder, T. R. Ray, A. Turnquist, S. B. Kim, N. Nyberg, A. Hourlier-Fargette, J. B. Model, A. J. Aranyosi, S. Xu, R. Ghaffari, J. A. Rogers, *ACS Sens.* **2019**, 4, 379.

- [107] R. Moreddu, M. Elsherif, H. Butt, D. Vigolo, A. K. Yetisen, *RSC Adv.* **2019**, *9*, 11433.
- [108] R. Moreddu, M. Elsherif, H. Adams, D. Moschou, M. F. Cordeiro, J. S. Wolffsohn, D. Vigolo, H. Butt, J. M. Cooper, A. K. Yetisen, *Lab Chip* **2020**, *20*, 3970.
- [109] S. A. Wade, S. F. Collins, G. W. Baxter, *J. Appl. Phys.* **2003**, *94*, 4743.
- [110] A. G. Bispo, S. A. M. Lima, L. D. Carlos, R. A. S. Ferreira, A. M. Pires, *J. Lumin.* **2020**, *224*, 117298.
- [111] N. J. van Eck, L. Waltman, *J. Informetr.* **2014**, *8*, 802.
- [112] N. J. van Eck, L. Waltman, *Scientometrics* **2017**, *111*, 1053.



João F. C. B. Ramalho got his M.Sc. in physics engineering at the University of Aveiro in 2016. In 2017, he started his Ph.D. at the University of Aveiro in the field of smart disposable labeling and real-time temperature sensing in the context of IoT, using organic–inorganic hybrid materials and QR codes. His main interests are in the fields of smart labeling, IoT, and luminescence thermometry.



Luís D. Carlos is a full professor in the Department of Physics at the University of Aveiro, Portugal. He is a member of the Lisbon Academy of Sciences and the Brazilian Academy of Sciences. He is editor of *Physica B—Condensed Matter*, *Physics Open*, special chief editor of *Frontiers in Chemistry (Inorganic Chemistry)*, associate editor of the *Journal of Luminescence*, and member of the editorial board of the *Journal of Sol-Gel Science and Technology*, *Journal of Rare Earths*, *Sensors*, *Results in Optics*, and *ChemPhotoChem*. His research interests include nanothermometry, organic/inorganic hybrids for green photonics, and optomagnetic nanomaterials.



Paulo S. André got a bachelor's in physics engineering (1996), a Ph.D. (2002) and an Agregação in physics from the Universidade de Aveiro, Portugal. He is full professor in the Department of Electrical and Computer Engineering at Instituto Superior Técnico, University of Lisbon and is senior researcher of the Instituto de Telecomunicações. He has published 230 papers, 550 communications, 20 books/books chapters and 10 patents. His current research interests include the study and simulation of photonic and optoelectronic components and systems, for sensing, communications, and energy applications. He is a senior member of the Institute of Electrical and Electronics Engineers.



Rute A. S. Ferreira is an associate professor with “Agregação” in the Department of Physics at the University of Aveiro and she is vice-director of CICECO—Aveiro Institute of materials. She is a member of the Scientific Council for Exact Sciences and Engineering of the Portuguese Science Foundation (FCT) and a member of the editorial board of *Materials Today*, *Advanced Photonics Research* and *ACS Omega*. Her current scientific interests are focused on organic/inorganic hybrids foreseeing applications in the fields of optoelectronics/green photonics (solid-state lighting, and integrated optics), photovoltaics (luminescent solar concentrators and down-shifting layers) and single ion or molecule magnet.